CFD-BASED ESTIMATION OF COLLISION PROBABILITIES BETWEEN FINE PARTICLES AND BUBBLES HAVING INTERMEDIATE REYNOLDS NUMBER

*M. NADEEM, J. AHMED, I.R. CHUGHTAI and ATTA ULLAH

Department of Chemical and Materials Engineering, PIEAS, P.O. Nilore, Islamabad, Pakistan

Recent literature comprises numerous investigations on the determination of bubble-particle collision probabilities in flotation systems based upon hydrodynamic models. This work aims to use CFD to simulate collision probabilities in quiescent flotation conditions as encountered in Flotation Columns. Euler-Lagrange approach is used for the calculation of collision probabilities of fine ($10\mu m$ to $80\mu m$) solid particles with bubbles having intermediate Reynolds number (i.e. $2<Re<500$; $0.1mm<d_b<1.5mm$). In this work only two bubble sizes, 1.0 mm and 1.5 mm, are simulated. The simulations are performed using both unstructured and structured meshes. The values of collision probabilities are compared with those produced using the hydrodynamic models of Yoon & Luttrell and Weber & Paddock. The results of collision probabilities and their variations with bubble and particle sizes, obtained using structured mesh are in close agreement with the published data.

Keywords: CFD, Collision probabilities, Flotation column

Nomenclature

C_D drag coefficient

d_b diameter of bubble

d_p diameter of particle

F_D drag force per unit particle mass

g gravitational acceleration

k turbulent kinetic energy

p pressure

Re Reynolds number

u velocity vector

u_p velocity of particle

u_t terminal velocity of bubble

ε dissipation rate

ρ density of fluid phase

ρ_p density of particle

ρ_s density of slurry

μ molecular viscosity

μ_{eff} dynamic viscosity

μ_L laminar viscosity

μ_T turbulent viscosity

τ stress tensor

1. Introduction

Column Flotation has become a widely acceptable technology in mineral processing industry. The need for successful design and scale-up has encouraged a significant amount of research to understand the sub-processes involved in flotation. The major sub-processes involved are the collision, attachment and retention of particles with bubbles. Among these sub-processes, the collision of bubble and particles is the most important phenomena effecting the flotation rate constant and recovery. The collision rate is usually expressed as bubble particle collision probability also known as collision efficiency. Finch and Dobby [1] has defined the probability of collision as the fraction of particles in the path of a bubble that actually collides with it. Collision probability is the function of the Stokes number, Reynolds number and the apparent particle settling velocity.

A large number of hydrodynamic models are available in literature to determine bubble particle collision probability. Cruz and Rubinstein [2, 3] have presented good reviews of these models. In these models, the flow pattern of liquid around a bubble is assumed to be in the form of streamlines and stream functions are derived for the location of a particle with respect to a bubble. These models

cover the entire range from Stokes flow to Potential flow conditions. In column flotation quiescent flow condition occurs with intermediate bubble Reynolds number. For intermediate bubble Reynolds number, the correlations developed by Weber and Paddock [4] and Yoon and Luttrell [5] are more representative of column flotation process. In recent years, CFD is being used for the modelling of the flotation systems. CFD modelling of the bubble-particle collision rates and efficiencies in the flotation cell has been performed [6].

The work presented in this paper aims at the CFD simulation of the bubble-particle collision probabilities between fine particles and bubbles of intermediate Reynolds number as exist in the flotation column [1]. The particle size range varies from 10μm to 80 μm and Reynolds number varies from 2 to 500. In this simulation the path of individual particle around the bubble is tracked and collision probability is determined by calculating the number of particles colliding with the bubble. This approach gives a direct method of determining the collision probability. In this work only two bubble sizes, 1.0 mm and 1.5 mm, are simulated.

2. Model Description

For the simulation of the bubble-particle collision probability Euler-Lagrange approach is used, in which Navier-Stokes equations have been solved for steady state. The fine particles are introduced as a discrete phase injection and solution has been obtained for the coupled flow. The tracks of fine particles have been determined to calculate collision probabilities.

2.1. Continuous phase modelling

For the continuous phase (water) steady state conservation equation of mass, momentum and turbulence are solved. For turbulence modelling k-ε model, most popular model for engineering application, is used. Following equations describe the conservation of mass and momentum for steady state:

$$\nabla \cdot \left(\rho \mathbf{u} \right) = 0 \tag{1}$$

$$\nabla \cdot \left(\rho \mathbf{u}\mathbf{u} \right) = -\nabla p + \nabla \cdot \left(\tau \right) + \rho \vec{g} \tag{2}$$

where τ is the effective stress tensor and expressed as

$$\tau = \mu_{eff} \left(\nabla \mathbf{u} + \left(\nabla \mathbf{u} \right)^T \right) \tag{3}$$

where effective viscosity is the sum of the laminar and turbulent viscosities:

$$\mu_{eff} = \mu_L + \mu_T \tag{4}$$

The standard k-ε model with standard wall functions has been used.

2.2. Trajectory calculations of fine particles

The trajectory of a discrete phase particle (fine particles) is predicted by integrating the force balance equation on the particle, which is written in a Lagrangian reference frame. This force balance equates the particle inertia with the forces acting on the particle, and can be written (for the x direction in Cartesian coordinates) as

$$\frac{du_p}{dt} = F_D \left(u - u_p \right) + \frac{g_x \left(\rho_p - \rho \right)}{\rho_p} + F_x \tag{5}$$

where $F_D \left(u - u_p \right)$ is the drag force per unit particle mass and

$$F_D = \frac{18\mu}{\rho_p d_p^2} \frac{C_D \, \text{Re}}{24} \tag{6}$$

Re is the relative Reynolds number, which is defined as

$$\text{Re} = \frac{\rho d_p \left| u_p - u \right|}{\mu} \tag{7}$$

The value of drag coefficient, C_D, can be obtained from literature. F_x incorporates additional forces in particle force balance like virtual mass force, the force required to accelerate the fluid surrounding the particle.

2.3. Numerical method

The commercial CFD code FLUENT 6 is selected to carry out the computer simulation. The calculation domain is divided into a finite number of control volumes. 2D segregated solver is chosen Pressure-velocity coupling is achieved by the SIMPLE algorithm. The first-order upwind

discretization scheme of momentum, turbulent kinetic energy and dissipation rate are chosen. In simulations, the standard values of the under-relaxation factors are used.

3. Simulations

In order to simulate the bubble particle collision probability in column flotation conditions, a small rectangular geometry is constructed with a stationary bubble at its centre. The liquid flows downward from the top of the column. It is assumed that solid particles move along the water (in the form of slurry) where as bubble rises upwards with their terminal velocities. Solid particles are also injected from the top having a velocity equal to the terminal velocity of the bubble plus the velocity of slurry.

The solid particles and bubbles move in opposite directions. The terminal velocity of bubble is calculated using the Intermediate law.

$$u_t = \frac{0.153 g^{0.71} d_b^{1.14} \left(\rho_s - \rho \right)^{0.7}}{\rho^{0.29} \mu^{0.43}} \qquad (8)$$

The approach used to determine collision probability in these simulations states that all particles moving downward in the vertically projected area above the bubble have the opportunity to collide with the bubble but due to the flow pattern around the bubble particles follow stream lines and very few of them actually collide with the bubble (Figure 1).The ratio of particles collided to the total number of particles gives collision probability
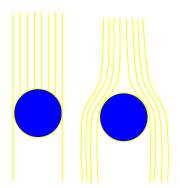

Figure 1.   Schematic diagram for collision probability; (a) bubbles having probability of collision; (b) bubbles that actually collide

The simulations are performed for different types of grid (i.e. unstructured grid and structured grid), which are discussed as follows:

3.1.   Case-I : Unstructured mesh

For the first simulation two small rectangular geometries having dimensions of 15x30 mm are constructed. The bubbles of diameter 1.0 mm and 1.5 mm are constructed at the centre of the geometry. Grid is constructed using GAMBIT mesh generator. The geometry is unstructured mesh with quadrilateral cell. The meshing of the geometry is shown in Figures 2 and 3.
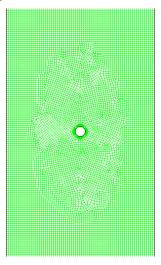

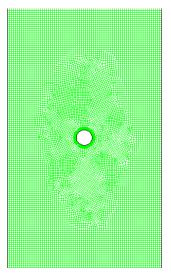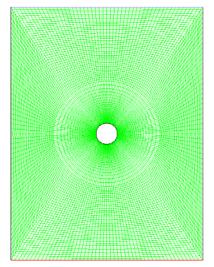Figure 2.   Schematic diagram of geometry for bubble of 1.0mm diameter with unstructured mesh.

Figure 3.   Schematic diagram of geometry for bubble of 1.5 mm diameter with unstructured mesh.

3.2. Case-II: structured mesh

In this case, a structured mesh is generated by dividing the geometry in small regions and meshing them. The whole geometry is divided into fourteen parts and each part is meshed separately to produce a structured mesh. The structured meshes are shown in Figures 4 and 5. The geometry dimensions are 9x12 mm and 13.5x18 mm for 1.0 mm and 1.5 mm bubble diameter respectively. These dimensions are selected to neglect the wall effect on the simulation.

Figure 4. Schematic diagram of geometry for bubble of 1.0 mm diameter with structured mesh.

Figure 5. Schematic diagram of geometry for bubble of 1.5 mm diameter with structured mesh.

4. Results

The simulations are performed for the initial conditions given in Table I. These initial conditions are same for both structured and unstructured meshes.

Table 1.   Modelling conditions.

Name of Parameter	Value for bubble diameter	
	1.0 mm	1.5 mm
Bubble terminal velocity , $m/\sec$	0.1068	0.1696
Reynolds number of bubble	107	254
Velocity of the slurry, $m/\sec$	0.005	0.005
Inlet velocity of the solid particle injections, $m/\sec$	0.1118	0.1746
Inlet turbulent intensity, %	10	10
Diameter of the particle, μm	10, 20,30,40,50, 60,70 and 80	

Trap boundary condition is set on the bubble so that when a particle collides with the bubble it is trapped on the bubble. The number of trapped particles is reported in the results and ratio of trapped particles to the total number of incident particles gives the collision probability.

The physical properties of the continuous phase are taken as of water and silica particles (2650 kg/m^3) are taken as discrete phase. Before particle tracking, simulation is conducted with single phase, i.e., water, to determine the velocity distribution of water. Then, silica particles of uniform size are injected through the inlet and their flow paths within the geometry are tracked using Discrete Phase Model (DPM) available in FLUENT 6. Simulation runs are repeated for silica particles of different size.

The velocity distribution of the water around the bubble is shown in Figures 6 and 7.
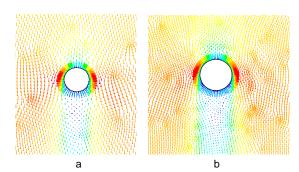

a   b

Figure 6. Velocity vectors around bubbles with unstructured mesh (a) 1.0 mm dia,; (b) 1.5 mm dia.
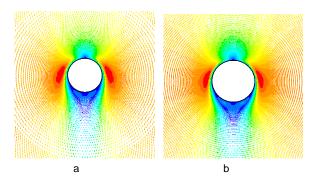
M. Nadeem et al.

Figure 7.   Velocity vectors around bubbles with structured mesh (a) 1.0 mm dia,; (b) 1.5 mm dia.

The comparison of velocity profiles around the bubble can be seen from Figures 6 and 7. The velocity of water is maximum at the sides of bubble and minimum at top of bubble where all water is stopped by the bubble and in the wake of bubble. Further, the structured mesh gives better presentation of velocity distribution than that of unstructured mesh.

The tracks followed by the particles of various diameters around the bubble of 1.0 mm diameter and 1.5 mm diameter for the simulation performed using unstructured grid are shown in Figure 8 and Figure 9 respectively. Figure 9 shows that small particles may be trapped in the wake of bubble de to their less inertia. These tracks are only for demonstration where as in actual simulations a large number of tracks have been used. For the simulations using structured mesh, particle tracks around the bubble are shown in Figures 10 and 11.
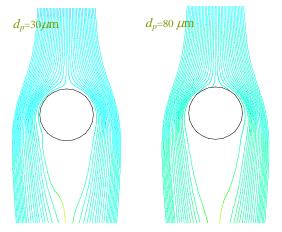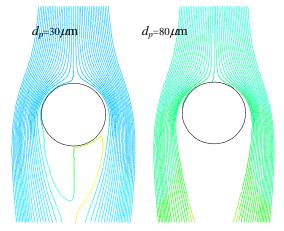

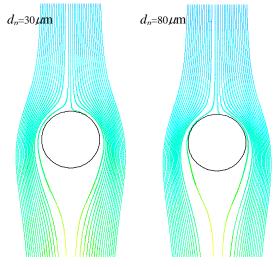Figure 9,   Tracks of particle streamlines around 1.5 mm diameter bubble with unstructured mesh.

Figure 10. Tracks of particle streamlines around 1.0 mm diameter bubble with structured mesh.

Figure 8.   Tracks of particle streamlines around 1.0 mm diameter bubble with unstructured mesh.
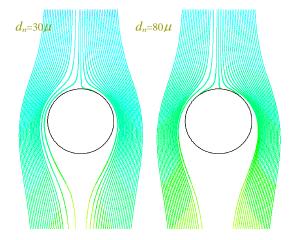

Figure 11. Tracks of particle streamlines around 1.5 mm diameter bubble with structured mesh.

The results of bubble particle collision probabilities for 1.0 mm diameter bubble calculated by this simulation are graphically represented in Figure 12 and those for 1.5 mm diameter are shown in Figure 13.

Based upon this numerical study the particles with diameter 30 μm or less follows the fluid streamlines due to less inertia and pass by the bubble without having any collision. However, in practice, these particles have some probability of collision with bubble.
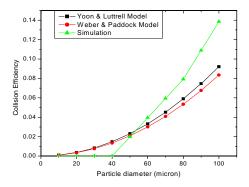

Figure 12. Comparison of the results of CFD simulations and hydrodynamic models for 1.0 mm bubble with unstructured mesh geometry.
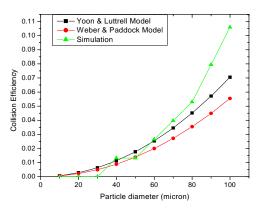

Figure 13. Comparison of the results of CFD simulations and hydrodynamic models for 1.5 mm bubble with unstructured mesh geometry.

These results are also compared with the results obtained from existing models of collision probability by Yoon and Luttrell [5] and by Weber and Paddock [4]. It is observed that estimated results are significantly different from published data.

Figure 14 represents the comparison of the simulation results obtained by using structured mesh for 1.0 mm diameter bubble with the hydrodynamic models of Yoon and Luttrell [5] and of Weber and Paddock [4]. These results are in better agreement with the results of Weber and Paddock [4]. The results obtained using structured mesh are better than that of unstructured mesh due the fact that it has better size control, better distribution and better orthogonality.
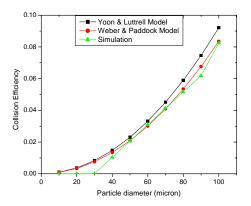

Figure 14. Comparison of the results of CFD simulations and hydrodynamic models for 1.0 mm bubble with structured mesh geometry.

Comparison of the simulation results obtained by using structured mesh for 1.5 mm diameter bubble with the hydrodynamic models is shown in Figure 15. In this simulation the particles with diameter of 10 μm and 20 μm do not collide with the bubble. The results for this simulation are in close agreement with the hydrodynamic model of Yoon and Luttrell [5]. The difference between the results of simulations and hydrodynamic models can be minimized by using a finer grid but it will add a lot to the computational effort required.
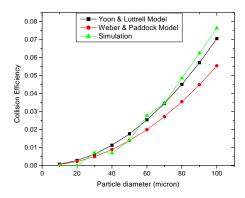

Figure 15. Comparison of the results of CFD simulations and hydrodynamic models for 1.5 mm bubble with structured mesh geometry.

The simulated values of collision probabilities for the bubble size of 1.0 mm and 1.5 mm are also

compared with each other. It is found that the collision efficiency values are higher for the smaller bubble than that of a larger bubble. This behavior is very much according to the expected results as large bubbles have higher values of terminal velocities. Figure 16 shows the variation of collision probability with particle diameter for different bubble sizes.
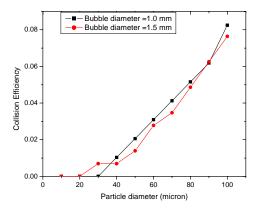

Figure 16. Comparison of collision probabilities for different bubble diameters with structured mesh geometry.

5.   Conclusions

The Euler-Lagrange approach is a useful CFD technique to determine the bubble particle collision probability. Further, the CFD simulations for the estimation of collision probabilities of fine particles with intermediate Reynolds number produced the results which are in agreement with those produced using existing hydrodynamic models for intermediate bubble Reynolds number. Finally, simulations performed with structured mesh produce better results than unstructured mesh.

References

[1]   J.A. Finch and G.S. Dobby, "Column Flotation", Pergamon Press, Oxford, (1990) p. 39-42.

[2]   E.B. Cruz, "A comprehensive dynamic model of the column flotation unit operation", PhD Dissertation, Virginia Polytechnic Institute and State University, Blacksburg, Virginia, (1997) p. 106-177.

[3]   J.B. Rubinstein, "Column Flotation" Taylor & Francis (1995) p. 155-164.

[4]   M.E. Weber and D. Paddock, J. Colloid Interface Sci. **94** (1983) 328.

[5]   R.H. Yoon and G.H. Luttrell, Miner. Process. Extr. Metall. Rev. **5** (1989) 101.

[6]   P.T.L. Koh and M.P. Schwarz, Miner. Eng., **16** (2003) 1055.